This is the accepted manuscript made available via CHORUS. The article has been published as:

Magnetic-Domain-Wall-Induced Electrical Polarization in Rare-Earth Iron Garnet Systems: A First-Principles Study

Temuujin Bayaraa, Changsong Xu, Yali Yang, Hongjun Xiang, and L. Bellaiche

Phys. Rev. Lett. **125**, 067602 — Published 7 August 2020

DOI: 10.1103/PhysRevLett.125.067602

Magnetic-domain-wall-induced electrical polarization in rare-earth iron garnet systems: A first-principle study

Temuujin Bayaraa[1], Changsong Xu[1,2*], Yali Yang[3], Hongjun Xiang[3,4,5], L. Bellaiche[1,2]

[1]Physics Department, University of Arkansas, Fayetteville, Arkansas 72701, United States
[2]Institute for Nanoscience and Engineering, University of Arkansas, Fayetteville, Arkansas 72701, United States
[3]State Key Laboratory of Surface Physics and Department of Physics, Fudan University, Shanghai 200433, China
[4]Collaborative Innovation Center of Advanced Microstructures, Nanjing 210093, China
[5] Shanghai Qi Zhi Institute, Shanghai 200232, China

Abstract

First-principles methods are employed to understand the existence of magnetic-domain-wall-induced electric polarization observed in rare-earth iron garnets. In contrast with previous beliefs, it is found that the occurrence of such polarization neither requires the local magnetic moments of the rare-earth ions nor non-collinear magnetism. It can rather be understood as originating from a magnetoelectric effect arising from ferromagnetic interactions between octahedral and tetrahedral Fe ions at the domain walls, and the mechanism behind is found to be a symmetric exchange-striction mechanism.

With the increasing demand for more information and data centers, the challenge for more computing power is rising, and with it, more power consumption. This trend is triggering an intense search for new energy-efficient technologies for information processing [1]. One possible solution would be the use of energy-efficient voltage control of magnetization through a magnetoelectric coupling. Therefore, magnetoelectric and multiferroic materials are attracting great interest in the spintronic community. Since the discovery of multiferroic properties, a number of materials have been found, however, the magnetoelectric coupling effect of these materials is either small or achievable at low cryogenic temperatures [2]. The search for high-temperature magnetoelectricity has led to new trends such as magnetoelectricity on the level of domain [3–5] and domain wall [6–14]. The magnetic domain walls (DW) are the natural interfaces between regions that are homogeneously magnetized, and it was indicated that Néel-type DW should have an electric polarization and react to an electric field [15]. Controlling the properties of DW offers great potential for technological applications such as memory devices, spintronics, and communications [8,16]. Recently, there have been reports of observation of a giant magnetoelectric effect in epitaxial rare-earth iron garnet films [15,17–20] and the use of this effect is demonstrated as optical nanoshutter in Ref. [21].

Note that, being magnetic and insulators, rare-earth iron garnets $Re_3Fe_5O_{12}$ (RIG) are also being studied extensively due to their many applicable properties [10,22–32]. Below the Néel temperature, there is a strong antiferromagnetic coupling between a non-equivalent number of Fe ions that occupy the tetrahedral and octahedral sites in a unit cell (ratio 3:2). Below the temperature that is the so-called "magnetization compensation temperature", rare-earth ions sitting at the dodecahedral sites develop a finite magnetic moment that is typically coupled antiferromagnetically with the tetrahedral Fe moment. Consequently, a ferrimagnetic ordering happens in RIGs [28,33].

Interestingly, the mechanism behind the aforementioned magnetoelectric effect in magnetic DW of RIGs [15,17–20] is still in dispute and there are several hypotheses: (i) Dzyaloshinskii-Moriya-like interactions [34] such as inhomogeneous magnetoelectric interaction due to the chirality of magnetic spin arrangements [20,35,36], or (ii) the local decompensation of the antiferroelectric structure in the DW, which involves rare-earth and iron ions exchange interaction [10,14,37]. One may also wonder what are the precise (hypothetical) contributions of tetrahedral and octahedral ions and of the Gd ions, and of their possible magnetic moments, as well as the oxygen ions on such electrical polarization.

In this work, we used a first-principles approach to further confirm that magnetic DW does possess an electric polarization in RIG systems, as well as, to resolve all the issues mentioned above. In particular, we reveal (1) that the magnetism of the rare-earth element is not crucial for this magnetoelectric effect; (2) which element is the main contributor to the electrical polarization; (3) that such polarization does not require the aforementioned items (i) and (ii) to occur, but rather can be simply explained by the specific collinear and symmetric exchange-striction mechanism that was also found to be behind the improper ferroelectricity of magnetic domains made of rare-earth orthoferrites [38].

Here, we mostly study 2x1x1 and 4x1x1 supercells of Gadolinium Iron Garnet (GIG) systems that have a DW in the middle (along the pseudo-cubic [100] a-axis) of these supercells. Figure 1 shows a simplified sketch of spin arrangements that are considered in the supercells that are

considered in this study. The gray area at the center represents the DW and the magnetic configuration inside each domain consists of tetrahedral Fe (Fe^{tet}) ions being arranged antiferromagnetically with respect to the other two sublattices (octahedral Fe, Fe^{oct}, and Gd ions) -- since it was reported to be the lowest energy collinear spin configuration for GIG bulk [25], in agreement with experiments [28,33]. As shown in Fig. 1, the two domains of the studied supercells have a magnetic configuration that is reversed with respect to each other and the *a* axis is the direction that is normal to the DW. All calculations are carried out within the framework of the density functional theory (DFT) as implemented in the Vienna *ab initio* simulation package (VASP) [39] using the projector augmented-wave potentials [40]. The following electrons are always treated as valence states: O 2*s* and 2*p*, and Fe 3*d*. On the other hand, we used two different schemes for the valence electrons of Gd: 4*f,* 5*s,* 5*p*, 5*d* and 6*s* where *f*-electrons are thus treated as valence electrons (and, consequently, magnetization arising from Gd ions can occur) *versus* "only" 5*p*, 5*d* and 6*s* where *f*-electrons are treated as core electrons and thus magnetic ordering of Gd ions is not accounted for. The generalized gradient approximation (GGA) together with the revised Perdew-Burke-Ernzerhof exchange-correlation functional for solids (PBEsol) [41] is employed with an effective Hubbard *U* parameter of 4eV for the localized *3d* electrons of Fe ions and U = 4eV for the localized *4f* electrons of Gd ions when these *4f* electrons are treated as valence electrons. Such values were demonstrated to provide accurate results [25,42–45]. We performed all our calculations at a collinear level, implying that spin-orbit effects (such as Dzyaloshinskii-Moriya-like interactions [46,47]) are not incorporated in the simulations. As we will see and at odds with previous beliefs [2,10,14,37,48], such choice does not prevent the occurrence of electrical polarization in the studied supercell. All structural degrees of freedom are allowed to relax. Moreover, the energy cutoff of 500 eV is used, and Monkhorst-Pack k-point mesh is chosen to be 2x4x4 for the 2x1x1 supercell and 1x4x4 for the 4x1x1 supercell. Structural relaxations are performed until the Hellmann-Feynman force on each atom is less than 0.005 eV/ Å, and the polarization is calculated by the Berry-phase method [49].

Table I reports the polarization of our studied GIG supercells when we consider or do not consider *f*-electrons of the Gd ions as valence electrons, which we denote as the "with-f" *versus* the "without-f" cases, respectively. It is remarkable that, in both cases and for both considered supercells, the existence of domain walls in GIG gives rise to a polarization -- which we further numerically found to develop along the normal to the DW, thus inducing an orthorhombic *Iba2* space group according to the FINDSYM software [50] (in addition to the above-mentioned supercell sizes, we also considered a supercell possessing GIG magnetic domains with the normal of DW lying now along the pseudo-cubic [110] direction and found a DW-induced polarization there along such normal too. In that case, the crystallographic space group is monoclinic *P2***)**. Such polarization is consistent with previous works on RIGS [2,10,14,15,35,37,48,51–61] and contrasts with the paraelectric nature of GIG monodomain.

It is important to realize that the "without-f" case also yields an electric polarization, which is more than twice as large as that of the "with-f" case. For example, the 4x1x1 supercell of GIG where *f*-electrons are considered as valence electrons has a total polarization of 0.001 C/m^2 but, when *f*-electrons are frozen as core electrons, the total polarization increases to 0.003 C/m^2 -- which is larger by one order of magnitude than the polarization typically induced in improper ferroelectrics (<100$\mu C/m^2$) [62–64]. Furthermore, one can see that the polarization of the 4x1x1

supercell is about half that of the 2x1x1 supercell in both cases (with and without *f*-electrons situations), which clearly confirms a DW-induced mechanism (an increase in the magnitude of the polarization with a decrease of the ratio of the DW volume over the total volume was also reported in Refs. [14,38]). The fact that the polarization survives and is even enhanced in the "without-f'' case with respect to the "with-f" situation automatically implies that the polarization in RIG systems does not have to mainly arise from the magnetism of rare-earth ions, which is in contrast to the assumption of Refs. [2,10,14,37,48]. To definitely assert such latter important point, we conducted similar calculations of 2x1x1 supercells made of Yttrium Iron Garnet (YIG) and Lutetium Iron Garnet (LuIG) systems and reported their results in Table I. Recalling that Yttrium and Lutetium have an empty f-shell and a filled f-shell, respectively, and therefore cannot possess magnetism. Thus, as revealed in Table I, the existence of polarization in the 2x1x1 supercells of YIG and LuIG systems (i) indeed emphasizes that the DW-induced polarization in RIGs does not originate from the magnetism of rare-earth ions, and (ii) it demonstrates that such polar effect should likely occur in any RIG systems with DW.

In order to gain insight into the mechanism responsible for this DW-induced polarization, we analyzed the atomic displacements of the relaxed 4x1x1 supercell structure of GIG with the DW at the center, with respect to its corresponding high-symmetry structure. Such 4x1x1 supercell is our largest studied supercell and can thus technically have the widest DW. All ions are found to have displacements along all three Cartesian directions, but with the net displacement of any type of ion along the direction that is *not* normal to the DW vanishing when averaging over the entire supercell. This is consistent with the Berry phase calculations not yielding any macroscopic polarization along the *b* and *c* directions. Regarding the ionic displacements along *a*-direction, results are shown at the top panels of Fig. 2. Any type of ion that is located near the DW center is getting largely displaced, unlike the ions that are located away from the DW. Note that octahedral Fe and O ions are displaced the most at the DW and that the Supplemental Materials provide further insight into the enhanced motions of octahedral Fe ions near the DW. We also computed the Fe^{oct}-O-Fe^{tet} angles (see Fig. 1 for the schematization of these angles) and report them on the bottom panels of Fig. 2 for both with (Panel c) and without *f*-electrons (Panel d) cases. They are also compared with the angles of 126.78º and 126.25º for both with and without *f*-electrons cases, respectively, that are found for a GIG *monodomain*. The Fe^{oct}-O-Fe^{tet} angle is changing significantly near the DW. In particular, this angle can be reduced by about 1.2-1.3 degrees from the aforementioned monodomain values when the involved octahedral and tetrahedral Fe ions are ferromagnetically (FM) coupled to each other at the DW (The magnetic interaction between first-nearest neighbor octahedral and tetrahedral Fe ions is the strongest among all interactions in GIG monodomain [45]). We further found that such decrease in the Fe^{oct}-O-Fe^{tet} angle is accompanied (i) by an increase in the distance between the octahedral and tetrahedral Fe ions at the DW and (ii) by the resulting fact that, among all oxygen ions, the ones involved in these angles at the DW are those that are displaced the most. We also estimated the ionic part of the polarization for the 4x1x1 supercell by multiplying the net displacement of each ion along the *a*-direction by its ideal ionic charge and report it in Figure 3. The estimated ionic parts associated with the polarization of Fe and Gd ions along the *a* have opposite signs and almost identical values, therefore nearly canceling each other. Thus, in the first approximation, the main contributor to polarization is found to be the O ions.

To reveal the mechanism behind this DW-induced polarization, we now use the unified model for the spin-order induced ferroelectricity [65–67]. Since we do not include spin-orbit coupling in our calculations, the spin-order-induced polarization can be written as $\vec{P} = \sum_{<i,j>} \vec{P}_{es}^{ij} \vec{S}_i \cdot \vec{S}_j$, where the summation is over all the spin pairs and $\vec{P}_{es}^{ij}$ is the polarization coefficient vector associated with the <i,j> spin pair. As Fig. 2 hints, this DW-induced electric polarization is likely linked to the ferromagnetic interaction between octahedral and tetrahedral Fe ions. As a result, we only take into account these ferromagnetic pairs in $\vec{P} = \sum_{<i,j>} \vec{P}_{es}^{ij} \vec{S}_i \cdot \vec{S}_j$. In order to calculate these $\vec{P}_{es}^{ij}$, we constructed a 160-atom supercell for a GIG system where *f*-electrons are treated as core electrons and with a DW at the center, due to heavy computational cost and to the fact that including *f*-electrons does not prevent the polarization from happening. We relaxed this supercell having a DW and then used the four-state energy mapping method [65,68] to find $\vec{P}_{es}^{ij}$ for all the ferromagnetic interactions between octahedral and tetrahedral Fe ions at the DW (which results in 12 $\vec{P}_{es}^{ij}$ involved in three different four-fold-degenerate-pairs). For all FM spin pairs at the DW, we thus let $\vec{S}_i \cdot \vec{S}_j = 1$. Our results for $\vec{P} = \sum_{<i,j>} \vec{P}_{es}^{ij} \vec{S}_i \cdot \vec{S}_j$ of the relaxed 160-atom supercell yield a net polarization of 0.01 C/m^2 along the *a* direction which is the direction normal to the DW (all other components vanish), which compares very well with the result from the Berry-phase method [49] of this supercell – which is found to be 0.0102 C/m^2. Such comparison, therefore, demonstrates the accuracy of our calculations and the validity of the model. The polarization results found here are about twice as larger as that of a 2x1x1 supercell (320 atoms supercell) shown in Table I since this latter has a smaller ratio of DW volume over the volume of the supercell. And the value of polarization is found to be inversely proportional to the size of the supercell, i.e. $\vec{P}_{nx1x1} = \vec{P}_{1x1x1}/n$. Furthermore, Figure 4 displays the corresponding $\vec{P}_{es}^{ij}$ (in blue color) along with the displacements of O ions (in red colors) that are involved in the ferromagnetic Fe^{oct}-O-Fe^{tet} angle at the DW. These $\vec{P}_{es}^{ij}$ and oxygen displacements are basically along the same direction for any of such oxygen ions. Such fact confirms that the displacements of O ions at the DW are the main contributors to the polarization (as a result of the ferromagnetic interaction between two types of Fe ions) and demonstrates that the symmetric exchange-striction mechanism described by $\vec{P} = \sum_{<i,j>} \vec{P}_{es}^{ij} \vec{S}_i \cdot \vec{S}_j$, is the mechanism behind the formation of electric polarization in RIGs. Overall, we show that the origin of the electric polarization in RIGs is due to the ferromagnetic interaction between octahedral and tetrahedral Fe ions at the DW that does not require complex explanations involving chirality or spin-orbit coupling. Furthermore, we used a simple model of magnetic DW to relate to experimental findings [18] and also show how our findings can be used in other domain wall types with continuous spin rotations, in the Supplemental Materials.

In summary, different supercells of rare-earth iron garnet systems with domain walls have been investigated via first-principle calculations. The main results are as follows: (1) all these supercells have a DW-induced electrical polarization along the direction of the normal of the domain walls; (2) such polarization neither requires the existence of magnetism at the rare-earth sites nor non-collinear magnetism to exist, in contrast to what was previously proposed. It rather originates from a (magnetoelectric) symmetric exchange-striction mechanism involving ferromagnetic interactions between octahedral and tetrahedral Fe ions at the DW. This latter mechanism takes the analytical form of $\vec{P} = \sum_{<i,j>} \vec{P}_{es}^{ij} \vec{S}_i \cdot \vec{S}_j$, which can also be used to

compute the electrical polarization for magnetic domains having a more realistic size than the ones chosen here (because of computational limitations). We hope that these findings provide a deeper understanding of magnetoelectricity, RIG systems, and domain wall engineering, and will encourage experimental confirmation using methods such as PUND (Positive Up Negative Down) [69] that is used in Ref. [70], or the Dielectric Leakage Current Compensation (DLCC) [71] and the Double-Wave Method (DMW) [72].

Acknowledgments

This work is supported by the Department of Energy, Office of Basic Energy Sciences, under Award No. DE-SC0002220

* cx002@uark.edu

	Supercell size		Polarization (mC/m^2)
GIG	2x1x1	with f	-2.133
		without f	-5.117
	4x1x1	with f	-1.100
		without f	-2.553
LuIG	2x1x1	filled f-shell	-2.458
YIG	2x1x1	empty f-shell	-2.157
GIG	1x1x2	with f	-2.250

Table I. Polarization (which lies along the *a*-axis) results of different supercells of RIG systems with DW at the center of the supercells.

Figure 1. Simple sketch of magnetic arrangement used for all supercells with DW at the center for RIG systems (Note that this sketch is a much-simplified version of the more complex magnetic interactions in RIG systems). Arrows represent the magnetic moments of both octahedral and tetrahedral Fe and Gd ions (in "without-f" case, spins at the Gd sites are not considered). The gray area in the middle and three dots at both ends represent the DW and continuation of magnetic arrangement within that domain.

Figure 2. DFT results for the GIG 4x1x1 supercell: Top panels (a,b) show the displacements of all ions along the *a* direction (which is normal to the DW) when *f*-electrons are treated as valence and core electrons, respectively; Bottom panels (c,d) show the Fe^{oct}-O-Fe^{tet} angles when *f*-electrons are treated as valence and core electrons, respectively. In panels c and d, "without DW" corresponds to Fe^{oct}-O-Fe^{tet} angles in a monodomain; "with DW and AFM" characterizes

the antiferromagnetic Fe^{oct}-O-Fe^{tet} angles in the multidomain; and "with DW and FM" display the ferromagnetic Fe^{oct}-O-Fe^{tet} angles in the multidomain.

Figure 3. Estimated contribution of each type of ion to the ionic part of the polarization along the *a* direction. Left and right sides are when *f*-electrons are treated as valence and core electrons, respectively.

Figure 4. The polarization coefficient vectors (blue) and displacement vectors (red) of the oxygen ions around the DW, having a normal along the *a*-axis, of a 160-atom supercell. The left panel concerns the (a,c) plane (thus possessing the DW's normal) while the right panel displays the (b,c) plane (that is thus perpendicular to the DW's normal). The "+" and "-" signs refer to the up and down directions of the magnetic moments of the Fe ions. The gray dashed line and purple arrows represent the DW region and direction of the electric polarization, respectively.

[1] A. Pyatakov, A. Kaminskiy, E. Lomov, W. Ren, S. Cao, and A. Zvezdin, SPIN **09**, 1940004 (2019).

[2] A. I. Popov, Z. V. Gareeva, F. A. Mazhitova, and R. A. Doroshenko, J. Magn. Magn. Mater. **461**, 128 (2018).

[3] Y. Geng, H. Das, A. L. Wysocki, X. Wang, S. W. Cheong, M. Mostovoy, C. J. Fennie, and W. Wu, Nat. Mater. **13**, 163 (2014).

[4] M. Matsubara, S. Manz, M. Mochizuki, T. Kubacka, A. Iyama, N. Aliouane, T. Kimura, S. L. Johnson, D. Meier, and M. Fiebig, Science (80-.). **348**, 1112 (2015).

[5] S. Matzen and S. Fusil, Comptes Rendus Phys. **16**, 227 (2015).

[6] M. Fiebig, T. Lottermoser, D. Fröhlich, A. V. Goltsev, and R. V. Pisarev, Nature **419**, 818 (2002).

[7] F. Kagawa, M. Mochizuki, Y. Onose, H. Murakawa, Y. Kaneko, N. Furukawa, and Y. Tokura, Phys. Rev. Lett. **102**, 057604 (2009).

[8] D. Meier, J. Phys. Condens. Matter **27**, 463003 (2015).

[9] T. Xu, T. Shimada, Y. Araki, J. Wang, and T. Kitamura, Nano Lett. **16**, 454 (2016).

[10] A. I. Popov, Z. V. Gareeva, and A. K. Zvezdin, Phys. Rev. B **92**, 144420 (2015).

[11] J. Fontcuberta, V. Skumryev, V. Laukhin, X. Granados, and E. K. H. Salje, Sci. Rep. **5**, 13784 (2015).

[12] I. P. Lobzenko, P. P. Goncharov, and N. V. Ter-Oganessian, J. Phys. Condens. Matter **27**, 246002 (2015).

[13] Z. V. Gareeva, O. Diéguez, J. Íñiguez, and A. K. Zvezdin, Phys. Status Solidi - Rapid Res. Lett. **10**, 209 (2016).

[14] A. I. Popov, K. A. Zvezdin, Z. V. Gareeva, F. A. Mazhitova, R. M. Vakhitov, A. R. Yumaguzin, and A. K. Zvezdin, J. Phys. Condens. Matter **28**, 456004 (2016).

[15] A. S. Logginov, G. A. Meshkov, A. V. Nikolaev, and A. P. Pyatakov, JETP Lett. **86**, 115 (2007).

[16] G. Catalan, J. Seidel, R. Ramesh, and J. F. Scott, Rev. Mod. Phys. **84**, 119 (2012).

[17] G. V. Arzamastseva, A. M. Balbashov, F. V. Lisovskii, E. G. Mansvetova, A. G. Temiryazev, and M. P. Temiryazeva, J. Exp. Theor. Phys. **120**, 687 (2015).

[18] A. P. Pyatakov, A. K. Zvezdin, A. M. Vlasov, A. S. Sergeev, D. A. Sechin, E. P. Nikolaeva, A. V. Nikolaev, H. Chou, S. J. Sun, and L. E. Calvet, in *Ferroelectrics* (Taylor & Francis Group , 2012), pp. 79–88.

[19] V. Koronovskyy and Y. Vakyla, Electron. Mater. Lett. **11**, 1028-1032 (2015).

[20] I. S. Veshchunov, S. V. Mironov, W. Magrini, V. S. Stolyarov, A. N. Rossolenko, V. A. Skidanov, J. B. Trebbia, A. I. Buzdin, P. Tamarat, and B. Lounis, Phys. Rev. Lett. **115**, 027601 (2015).

[21] N. E. Khokhlov, A. E. Khramova, E. P. Nikolaeva, T. B. Kosykh, A. V. Nikolaev, A. K. Zvezdin, A. P. Pyatakov, and V. I. Belotelov, Sci. Rep. **7**, 264 (2017).

[22] E. R. Rosenberg, L. Beran, C. O. Avci, C. Zeledon, B. Song, C. Gonzalez-Fuentes, J. Mendil, P.

Gambardella, M. Veis, C. Garcia, G. S. D. Beach, and C. A. Ross, Phys. Rev. Mater. **2**, 094405 (2018).

[23] K. Shen, Phys. Rev. B **99**, 024417 (2019).

[24] S. Geprägs, A. Kehlberger, F. Della Coletta, Z. Qiu, E.-J. Guo, T. Schulz, C. Mix, S. Meyer, A. Kamra, M. Althammer, H. Huebl, G. Jakob, Y. Ohnuma, H. Adachi, J. Barker, S. Maekawa, G. E. W. Bauer, E. Saitoh, R. Gross, S. T. B. Goennenwein, and M. Kläui, Nat. Commun. **7**, 10452 (2016).

[25] R. Nakamoto, B. Xu, C. Xu, H. Xu, and L. Bellaiche, Phys. Rev. B **95**, 024434 (2017).

[26] S. Geller, J. P. Remeika, R. C. Sherwood, H. J. Williams, and G. P. Espinosa, Phys. Rev. **137**, A1034 (1965).

[27] S. M. Zanjani and M. C. Onbasli, AIP Adv. **9**, 035024 (2019).

[28] M. Deb, P. Molho, B. Barbara, and J.-Y. Bigot, Phys. Rev. B **97**, 134419 (2018).

[29] E. Sawatzky and E. Kay, J. Appl. Phys. **40**, 1460 (1969).

[30] E. Sawatzky and E. Kay, J. Appl. Phys. **42**, 367 (1971).

[31] M. Oron, I. Barlow, and W. F. Traber, J. Mater. Sci. **4**, 271 (1969).

[32] D. Bloch, F. Chaissé, and R. Pauthenet, J. Appl. Phys. **38**, 1029 (1967).

[33] W. Haubenreisser, Krist. Und Tech. **14**, 1490 (1979).

[34] S. W. Cheong and M. Mostovoy, Nat. Mater. **6**, 13 (2007).

[35] A. P. Pyatakov, D. A. Sechin, A. S. Sergeev, A. V. Nikolaev, E. P. Nikolaeva, A. S. Logginov, and A. K. Zvezdin, EPL **93**, 17001 (2011).

[36] D. P. Kulikova, T. T. Gareev, E. P. Nikolaeva, T. B. Kosykh, A. V. Nikolaev, Z. A. Pyatakova, A. K. Zvezdin, and A. P. Pyatakov, Phys. Status Solidi - Rapid Res. Lett. **12**, 1800066 (2018).

[37] A. I. Popov, D. I. Plokhov, and A. K. Zvezdin, Phys. Rev. B **90**, 214427 (2014).

[38] Y. Yang, H. Xiang, H. Zhao, A. Stroppa, J. Zhang, S. Cao, J. Íñiguez, L. Bellaiche, and W. Ren, Phys. Rev. B **96**, 104431 (2017).

[39] G. Kresse and D. Joubert, Phys. Rev. B **59**, 1758 (1999).

[40] P. E. Blöchl, Phys. Rev. B **50**, 17953 (1994).

[41] J. P. Perdew, A. Ruzsinszky, G. I. Csonka, O. A. Vydrov, G. E. Scuseria, L. A. Constantin, X. Zhou, and K. Burke, Phys. Rev. Lett. **100**, 136406 (2008).

[42] H. J. Zhao, J. Íñiguez, X. M. Chen, and L. Bellaiche, Phys. Rev. B **93**, 014417 (2016).

[43] O. Diéguez, O. E. González-Vázquez, J. C. Wojdeł, and J. Íñiguez, Phys. Rev. B **83**, 094105 (2011).

[44] C. Xu, Y. Yang, S. Wang, W. Duan, B. Gu, and L. Bellaiche, Phys. Rev. B **89**, 205122 (2014).

[45] T. Bayaraa, C. Xu, D. Campbell, and L. Bellaiche, Phys. Rev. B **100**, 214412 (2019).

[46] T. Moriya, Phys. Rev. **120**, 91 (1960).

[47] I. E. Dzyaloshinskii, Sov. Phys. JETP **10**, 628 (1960).

[48] A. I. Popov, Z. V. Gareeva, A. K. Zvezdin, T. T. Gareev, A. S. Sergeev, and A. P. Pyatakov, Ferroelectrics **509**, 32 (2017).

[49] R. D. King-Smith and D. Vanderbilt, Phys. Rev. B **47**, 1651 (1993).

[50] H. T. Stokes and D. M. Hatch, J. Appl. Cryst. J. Appl. Cryst **38**, 237 (2005).

[51] N. Hur, S. Park, S. Guha, A. Borissov, V. Kiryukhin, and S. W. Cheong, Appl. Phys. Lett. **87**, 042901 (2005).

[52] M. Mercier, Proc. Symp. Magnetoelectric Interact. Phenom. Crystals, Seattle, Wash, USA (1973).

[53] M. J. Cardwell, Phys. Status Solidi **45**, 597 (1971).

[54] S. Hirakata, M. Tanaka, K. Kohn, E. Kita, K. Siratori, S. Kimura, and A. Tasaki, J. Phys. Soc. Japan **60**, 294 (1991).

[55] H. Ogawa, E. Kita, Y. Mochida, K. Kohn, S. Kimura, A. Tasaki, and K. Siratori, J. Phys. Soc. Japan **56**, 452 (1987).

[56] R. V Pisarev, B. B. Krichevtsov, V. N. Gridnev, V. P. Klin, D. Frohlich, and C. Pahlke-Lerch, J. Phys. Condens. Matter **5**, 8621 (1993).

[57] V. E. Koronovskyy, S. M. Ryabchenko, and V. F. Kovalenko, Phys. Rev. B **71**, 172402 (2005).

[58] Y. Kohara, Y. Yamasaki, Y. Onose, and Y. Tokura, Phys. Rev. B **82**, 104419 (2010).

[59] A. S. Logginov, G. A. Meshkov, A. V. Nikolaev, E. P. Nikolaeva, A. P. Pyatakov, and A. K. Zvezdin, Appl. Phys. Lett. **93**, 182510 (2008).

[60] A. P. Pyatakov, G. A. Meshkov, and A. K. Zvezdin, in *J. Magn. Magn. Mater.* (2012), pp. 3551–3554.

[61] I. S. Veshchunov, S. V. Mironov, W. Magrini, V. S. Stolyarov, A. N. Rossolenko, V. A. Skidanov, J.-B. Trebbia, A. I. Buzdin, P. Tamarat, and B. Lounis, Phys. Rev. Lett. **115**, 027601 (2015).

[62] T. Kimura, T. Goto, H. Shintani, K. Ishizaka, T. Arima, and Y. Tokura, Nature **426**, 55 (2003).

[63] T. Kimura, G. Lawes, T. Goto, Y. Tokura, and A. P. Ramirez, Phys. Rev. B - Condens. Matter Mater. Phys. **71**, 224425 (2005).

[64] Y. Naito, K. Sato, Y. Yasui, Y. Kobayashi, Y. Kobayashi, and M. Sato, J. Phys. Soc. Japan **76**, 023708 (2007).

[65] H. J. Xiang, E. J. Kan, S.-H. Wei, M.-H. Whangbo, and X. G. Gong, Phys. Rev. B **84**, 224429 (2011).

[66] H. J. Xiang, E. J. Kan, Y. Zhang, M. H. Whangbo, and X. G. Gong, Phys. Rev. Lett. **107**, 157202 (2011).

[67] X. Z. Lu, M.-H. Whangbo, S. Dong, X. G. Gong, and H. J. Xiang, Phys. Rev. Lett. **108**, 187204 (2012).

[68] H. Xiang, C. Lee, H.-J. Koo, X. Gong, and M.-H. Whangbo, Dalt. Trans. **42**, 823 (2013).

[69] J. F. Scott, L. Kammerdiner, M. Parris, S. Traynor, V. Ottenbacher, A. Shawabkeh, and W. F. Oliver, J. Appl. Phys. **64**, 787 (1988).

[70] T. T. Gao, T. L. Sun, X. Q. Liu, H. Y. Zhou, H. Tian, L. Bellaiche, and X. M. Chen, Appl. Phys. Lett. **114**, 212904 (2019).

[71] R. Meyer, R. Waser, K. Prume, T. Schmitz, and S. Tiedke, Appl. Phys. Lett. **86**, 142907 (2005).

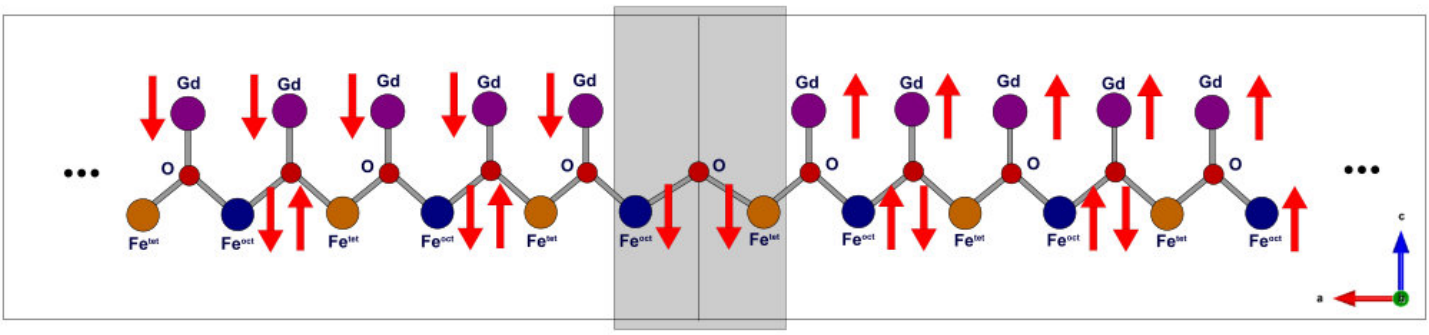
[72] M. Fukunaga and Y. Noda, J. Phys. Soc. Japan **77**, 064706 (2008).

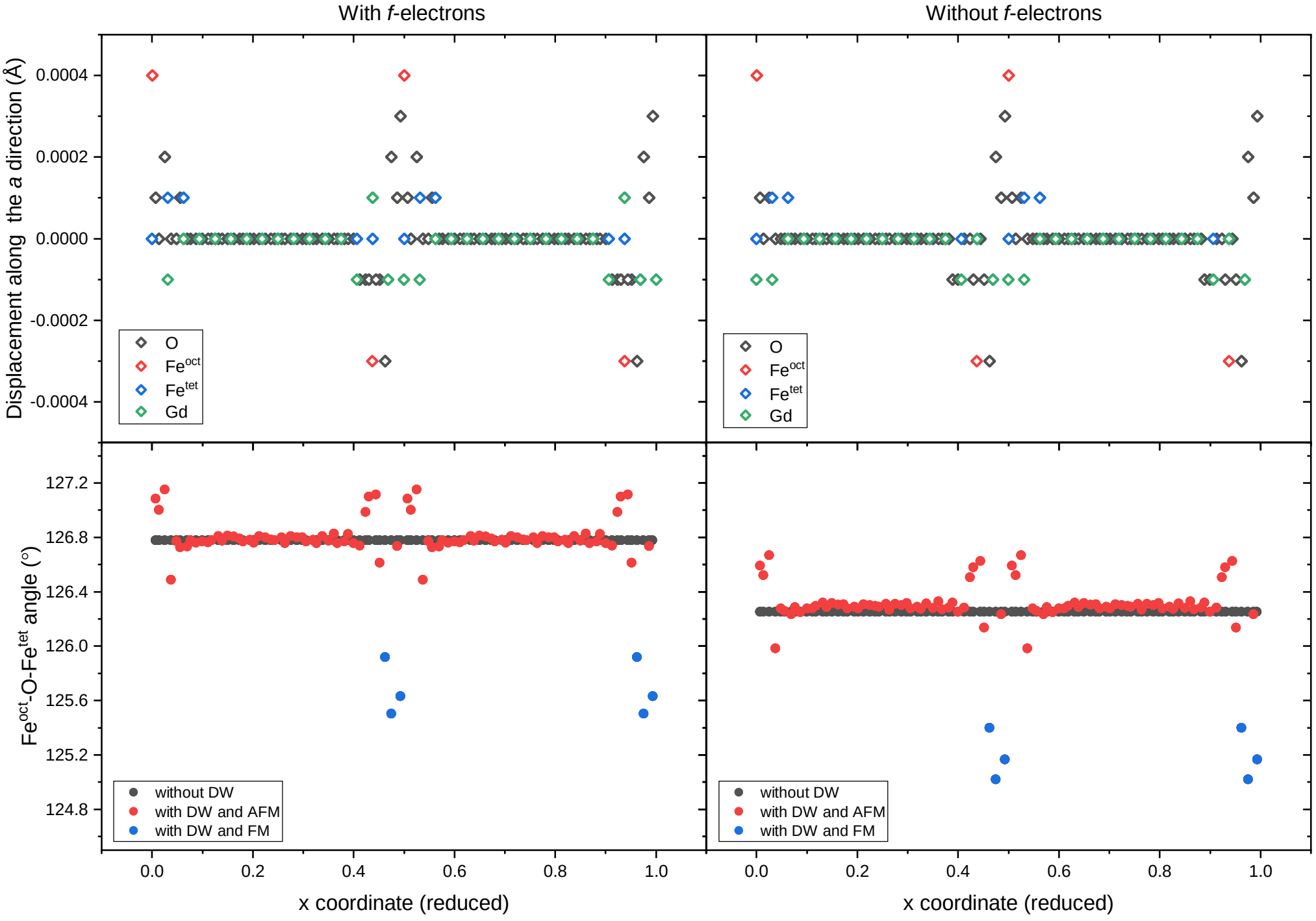
[73] See Supplemental Material [url] for (i) understanding of the displacement of the octahedral Fe ions at the DW; (ii) how a simple model of DW can be used to relate with experimental findings; and (iii) how our findings can also be employed to treat other DW types exhibiting continuous spin rotations, which includes Refs. [74-76].

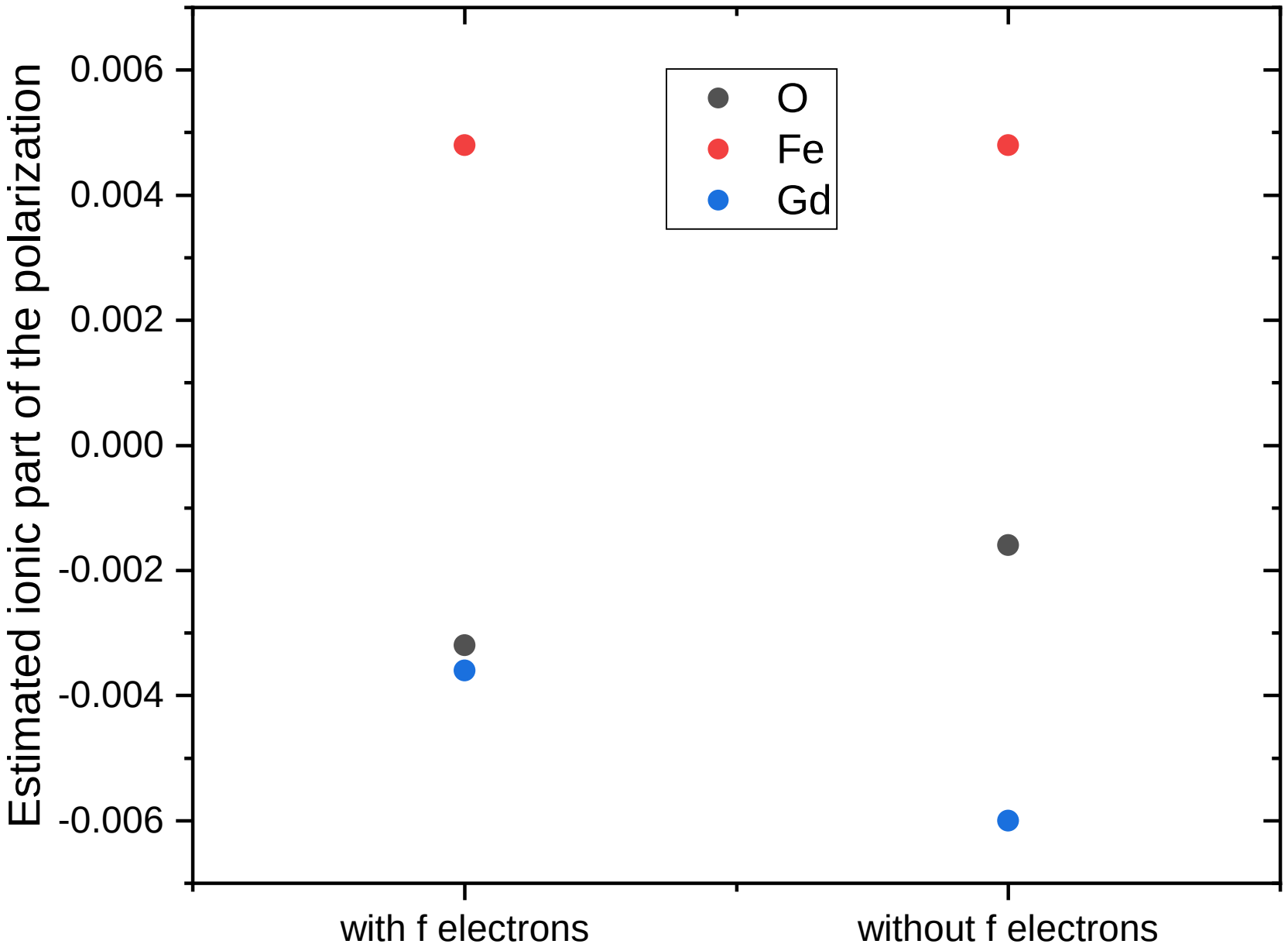
[74] Yang See-Hun and Parkin Stuart, J. Phys. Condens. Matter. **29**, 303001 (2017).

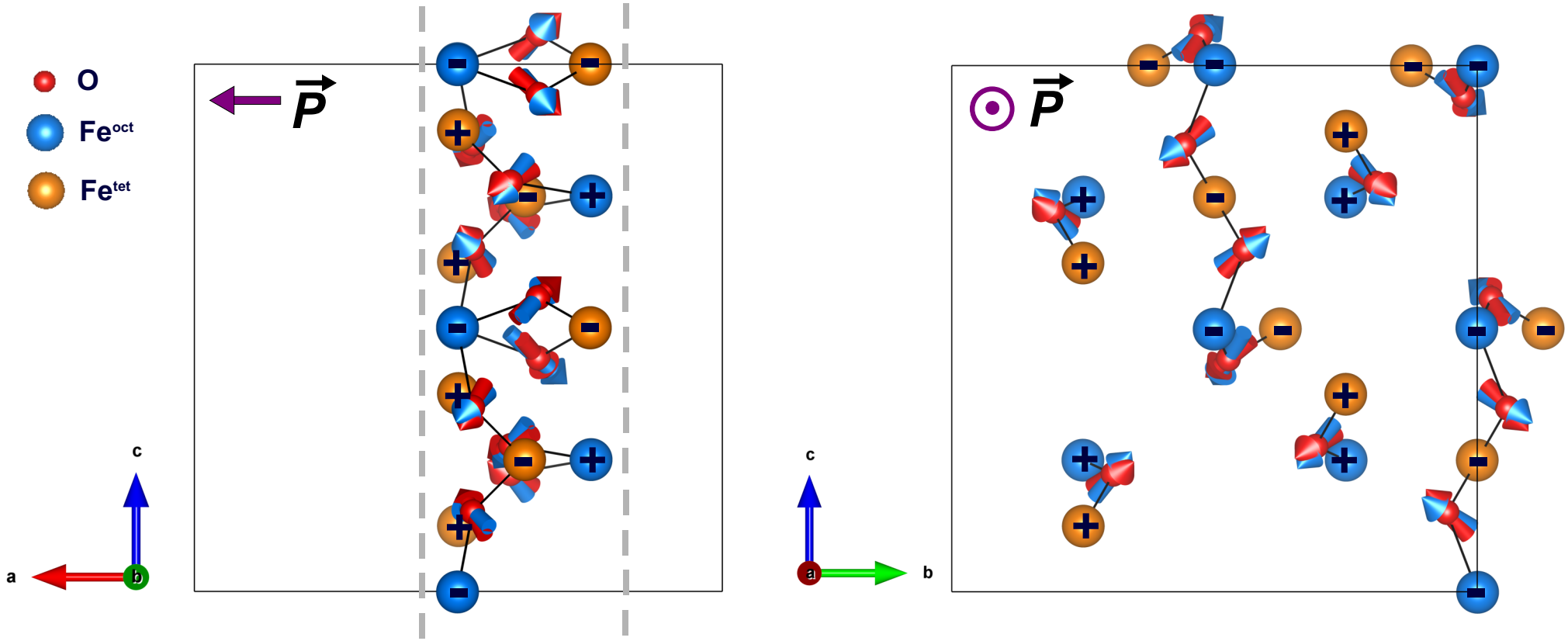
[75] Z. Yu, C. Wei, F. Yi, and R. Xiong, Nanomaterials **9**, 1538 (2019).

[76] S. H. Yang, K. S. Ryu, and S. Parkin, Nat. Nanotechnol. **10**, 221 (2015).


Gd
O
Fe^tet
Fe^oct
c
a


With f-electrons
Without f-electrons
Displacement along the a direction (Å)
0.0004
0.0002
0.0000
-0.0002
-0.0004
O
Fe^oct
Fe^tet
Gd
Fe^oct-O-Fe^tet angle (°)
127.2
126.8
126.4
126.0
125.6
125.2
124.8
without DW
with DW and AFM
with DW and FM
0.0
0.2
0.4
0.6
0.8
1.0
x coordinate (reduced)


Estimated ionic part of the polarization
0.006
0.004
0.002
0.000
-0.002
-0.004
-0.006
O
Fe
Gd
with f electrons
without f electrons


O
Fe^oct
Fe^tet
P
c
a
b
P
c
a
b